DOI: 10.54254/2753-8818/2026.33628

Comparative Analysis of Integrated Optical Electric Field Sensors: Configuration Design and Functional Performance

Zhuoxi Leng

College of Logistics Engineering, Shanghai Maritime University, Shanghai, China
202310232055@stu.shmtu.edu.cn

Abstract. The integrated optical waveguide electric field sensor (IOES) is a necessary measurement technology for power system monitoring, electromagnetic compatibility testing and military defense, which has excellent electromagnetic interference immunity, ultra-wide bandwidth and high sensitivity. The sensing ability and the modulation properties are reviewed for various architectures, such as the Mach–Zehnder interferometer (MZI), Michelson interferometer (MI) and micro-ring resonator (MRR). This part reviews an important obstacle in practice, that is, stability on the operating point against DC drift, which overcomes the transition from bulk lithium niobate material platform to the high refractive index contrast thin-film lithium niobate (TFLN) material platform. The following part reviews IOES performance and implementation methods for stabilization control means, such as asymmetric waveguide structure and the wavelength shifting mode. Finally, this paper outlines the future possible development directions for 3D vector detection and fully integrated photonic integrated circuits (PICs). However, this review is also a technical reference for designers in their endeavor of developing the next generation of high-performance electric field sensors in a complex electromagnetic environment.

Keywords: Integrated Optical Waveguide Electric Field Sensor, Electro-Optic Modulation, Mach–Zehnder Interferometer, Michelson Interferometer, Micro-Ring Resonator.

1. Introduction

Further requirements for ultra-high-performance metrology come with the advances of the Internet of Things technology, 5G/6G communications, the high-voltage smart grids, and so on. Enhancement of intelligent perception to observe electromagnetic environment is needed and has become more and more complex, which are facing stringent requirements of metrology for high-performance. In civil fields, the operating frequency band of the 5G communications expands to the millimeter-wave frequency band, demanding the electromagnetic compatibility (EMC) test equipment to have an extremely wide bandwidth and a high-frequency response [1,2]. Meanwhile, in the case of high-voltage power, real time monitoring of the transient voltage and lightning strike pulse is crucial for safe operation of the power grid. In military and national defense fields, the early warning and protection for high-power microwave (HPM) weapon and nuclear electromagnetic pulse (NEMP) need high fidelity detection of a strong electromagnetic pulse (EMP) detection equipment without imparting field distortion. The traditional electric field sensor type is divided into

DOI: 10.54254/2753-8818/2026.33628

two types: mechanical and electrical types. Mechanical-based sensors achieve sensing by measuring the mechanical deformation of sensing devices produced by electric fields. Although mechanical-based sensors have simple structures, their response speed is limited by the mechanical vibration speed (usually below kHz), which makes them unsuitable for high-frequency electric field detection. Electrical-based sensors (field mills, D-dot sensors, for example) have been matured, but their metal electrodes unavoidably warp the original electric field. In addition, D-dot sensors generally need integrated circuit integrator, limiting the accuracy and bandwidth of its time-domain measuring results [3].

But in integrated optical electric field sensors (IOES), significant technical advantages of the frequency response and field transparency also exist. The IOES adopts the Pockels effect of electro-optic crystal to directly modulate spatial electric field signal onto the optical carrier. It can be made of all-passive dielectric material like lithium niobate, so IOES not only causes little disturbance to the electric field being measured and has extremely high response frequency (theoretically THz) but also possesses great electromagnetic interference immunity [4]. Most of the electro-optic crystals such as lithium niobate (LN) are the substrate materials of the integrated optical sensor due to their large first order linear electro-optic coefficient (r_{33}). In recent years, integrated optical electric field sensors have undergone a breakthrough transition from bulk LN to thin-film lithium niobate (TFLN) platform [5].

Conventional Bulk LN devices are weak at light field confinement because of low refractive index contrast, resulting in a bending radius of the millimeter scale order and large chip size. Meanwhile, TFLN can bend the fiber to a micron-sized bending radius and achieve extremely small chip mode area by virtue of very high refractive index contrast, which not only greatly reduces device volume (such as from centimeter scale to 3.5 mm × 2 mm) but also greatly improves electro-optic modulation efficiency and response bandwidth. For the structure of sensors, it can also synthesize a variety of structures. From the traditional Mach–Zehnder interferometer (MZI) structure to the reflective Michelson interferometer (MI) structure, and then, the super-sensitive micro-ring resonator (MRR) structure, etc. all these structures are optimized for different applications, on the order of μV/m or MV/m intensity field sensitivity.

Going forward, as the sensor platform advances to high-integration TFLN, engineering implementation is only restricted by the stability of operating points. The generating characteristic of DC drift in the material of lithium niobate, changing external ambient temperature and stress, will cause the operating point of the sensor to be shifted, thus leading to the distortion of the tested signal nonlinearly. To this end, the authors proposed a stable control scheme based on asymmetric waveguide structures and wavelength-tunable feedback to achieve precise phase-bias lock for linearity performance in complex circumstances. First, it is introduced to the basic physical principle and features of electric field sensing; then it introduces evolution of interferometer and resonant sensing structure, respectively; afterwards, it introduces in detail the various feature parameters and application process of integrated optical waveguide electric field sensor; and last but not least, it indicates future development trends (detection of 3D electric vector and PIC).

2. Principle of integrated optical electric field sensing

The principle of IOES is the linear electro-optic effect (Pockels effect) of electro-optic crystals. Utilizing specific waveguide structures, it can transform spatial electric fields relatively difficult to sense directly into optical signals that are relatively easy to detect.

DOI: 10.54254/2753-8818/2026.33628

2.1. Linear electro-optic effect (pockels effect)

Essential working principle of IOES is Pockels effect (i.e., the first-order linear electro-optic effect). When an external electric field is applied to an electro-optic crystal (such as lithium niobate), its elliptical refractive index ellipsoid will be deformed. This affects its refractive index for light passing through this crystal, achieving phase modulation of light [6].

For the common x-cut y-propagation lithium niobate waveguide, light waves are propagating in its y direction. The relation between the refractive index changes Δn of light waves and the electric field strength E applied to lithium niobate can be expressed as:

$$\Delta n = \frac{1}{2} n_{\epsilon}^{3} r_{33} \Gamma E \tag{1}$$

E is the extraordinary index of the crystal outside electric field. r_{33} is the largest electrooptic coefficient of lithium niobate (roughly 30.9 pm/V); Γ is the overlapping factor of modulated electric field and optical field mode.

2.2. Interferometric sensing structure

Phase-modulated signals cannot be read directly by photodetector, so an interferometer structure is needed to convert the phase-modulated signals into intensity modulation.

The MZI is the most widely studied and mature structure among all available configurations. Optical beam is split into two paths of a Y-branch, and passes through the reference arm and the sensing arm respectively, with the sensing arm modulated by the electric field to generate phase difference. After, the two optical waves are concatenated together and interfered at the end of output. Figure 1 shows the schematic diagram of MZI structure.

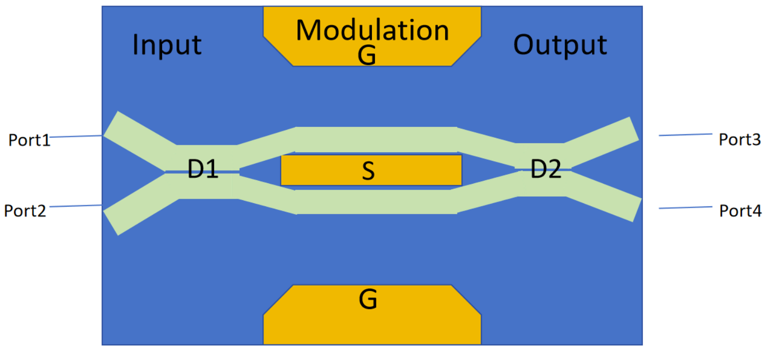

Figure 1. Schematic diagram of MZI structure

The end of the waveguide has a highly reflecting film or a Bragg grating, so the optical signal passes back and forth twice in the sensing arm. Compared with MZI, MI can realize twice the optical path difference for the same length, which will improve the modulation efficiency and the sensitivity of MI. It is also conducive to more compact device packaging. Figure 2 shows the schematic diagram of MI structure.

DOI: 10.54254/2753-8818/2026.33628

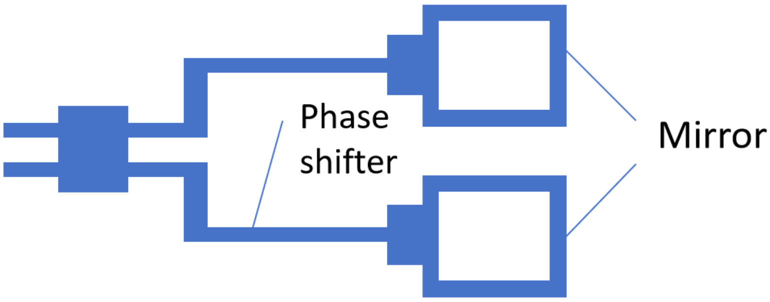

Figure 2. Schematic diagram of MI structure

The transfer function of an interferometric sensor is usually a cosine function:

$$P_{out} = \frac{1}{2}\alpha P_{in}\left[1 + k\cos(\phi(E) + \Delta\phi_0)\right] \tag{2}$$

Where αrepresents the system loss, $k$is the extinction ratio, and $\Delta\phi_0$denotes the intrinsic phase difference between the two arms. To achieve the maximum linear measurement range and sensitivity, the sensor needs to operate at the "linear point" (i.e., $\Delta\phi_0 = \pi/2$) through asymmetric waveguide design or bias control.

2.3. Resonant sensing structure

Resonant cavity structures (such as MRR) enhance the response through multiple circulating propagations of light within the ring waveguide. The sensing principle relies on the electric-field-induced refractive index change, which shifts the resonance wavelength of the cavity.

Compared with interferometric structures, resonant sensors exhibit extremely high sensitivity and smaller dimensions. However, its operating bandwidth is usually narrow, and it is extremely sensitive to fluctuations in ambient temperature, making stable control of its operating point quite difficult. Figure 3 shows the schematic diagram of MRR structure.

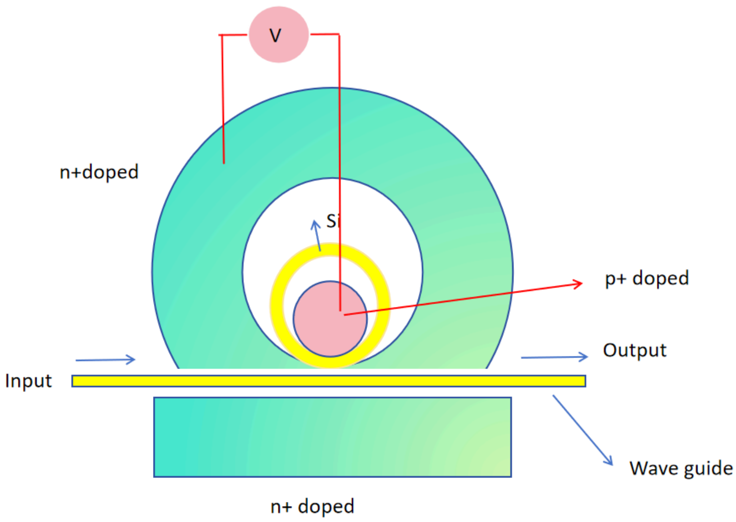

Figure 3. Schematic diagram of MRR structure

DOI: 10.54254/2753-8818/2026.33628

2.4. Antenna induction and field enhancement

To sense the spatial electric field, IOES usually integrates a metal induction antenna (such as a conical dipole antenna) near the sensing arm. The antenna senses the spatial electric field and generates an induced voltage between the modulation electrodes.

$$V = h_{eff} E \tag{3}$$

where h_{eff} represents the effective length. The local electric field generated by this voltage acts directly on the sensing waveguide. The geometric dimensions of the antenna (such as height h and width w) not only determine the frequency response range (bandwidth) of the sensor, but also directly affect the detection sensitivity of the sensor through its field enhancement factor F. The TFLN platform, with its stronger optical confinement, enables narrower electrode gaps, which produces a stronger local modulation field for the same applied voltage.

2.5. Performance parameters

2.5.1. Operating bandwidth

The operating bandwidth is defined as the spatial electric field frequency range corresponding to the point at which the system output response decreases by 3 dB.

It determines the sensor's ability to capture rapidly changing electromagnetic pulses (such as NEMP with nanosecond-level rising edges).

The theoretical bandwidth of sensors based on TFLN can reach 27.5 GHz or even more than 30 GHz [1]. Its actual bandwidth is mainly limited by the antenna induction efficiency, the frequency response of electrode modulation, and the velocity mismatch effect.

2.5.2. Half-wave electric field, $E\pi$

The half-wave electric field is a physical quantity analogous to the "half-wave voltage" of electro-optic modulators, describing the applied electric field intensity required to generate a π phase difference between the two arms of the sensor interferometer.

Calculation formula:

$$E_\pi = \frac{\lambda G_{el}}{n_e^3 r_{33} \Gamma G L_{el}} \tag{4}$$

where λ is the wavelength, G_{el} is the electrode spacing, L_{el} is the modulation length, Γ is the electro-optic overlap factor, and G is the antenna gain.

E_π directly determines the sensitivity and measurement range of the sensor. A smaller E_π corresponds to high sensitivity, while a larger E_π (e.g., on the order of MV/m) allows the sensor to operate without waveform distortion in strong electric field environments (such as 726 kV/m).

2.5.3. Sensitivity / minimum detectable field

Sensitivity is usually defined as the minimum spatial electric field intensity when the signal-to-noise ratio (SNR) is 1 (theoretical) or the output signal is 10 dB above the noise floor. It can be affected by system noise (thermal noise, shot noise, laser RIN noise), device extinction ratio (ER), and link gain.

DOI: 10.54254/2753-8818/2026.33628

2.5.4. Linearity & 1 dB compression point

High-sensitivity bulk material LN sensors can reach approximately 0.93 mV/m in the GHz band, while strong-field TFLN sensors exhibit lower sensitivity, at around the V/m order of magnitude.

1 dB compression point (IE1dB) is defined as the input electric field strength corresponding to the point at which the system output deviates from the linear response by 1 dB. It characterizes the maximum measurable field strength of the sensor without severe nonlinear distortion, with a theoretical value of approximately $0.297E_{\pi}$ [1].

2.5.5. Linear dynamic range (LDR)

LDR is the ratio (usually expressed in dB) between the minimum detectable field and the 1-dB compression point.

Theoretical derivation shows that the dynamic range of an electric field sensing system is independent of E_π and mainly depends on the noise level of the system and the gain of the optical link.

2.5.6. Field enhancement factor (Γ)

Γ is the ratio between the induced electric field between the modulation electrodes and the incident field from the outside world. By optimizing the antenna geometry (such as the height h and bottom width w) field strength, the enhancement factor can be maximized to obtain the voltage sensitivity of the sensor in targeted frequency ranges without changing the optical path.

2.5.7. Extinction ratio (ER)

ER is the ratio of the maximum optical power to minimum optical power of an output interferometer. A high ER (for example, greater than 30 dB) directly dictates the modulation depth and is the sole condition on the SNR and measurement accuracy of the device. Constraint by manufacturing tolerances and sidewall scattering in etch processes, TFLN devices typically have a slightly lower ER than bulk device materials.

2.5.8. Insertion loss (IL)

IL is the optical power attenuation when light propagates through the sensor, such as waveguide transmission loss, bending loss and fiber-coupling loss, and low insertion loss reduces the noise floor and the spurious-free dynamic range (SFDR) of the system. For an asymmetric structure, loss balance needs to be considered closely to avoid degradation of extinction ratio and maintain the stable phase bias.

3. Application progress of integrated optical waveguide electric field sensor

The all-dielectric nature and its electromagnetic transparency make IOES easily apply to power system monitoring, military, biomedicine and EMC related testing. According to differences of sensing structures, different configurations are established for practical metrology with various needs from μV/m level sensitivity down to MV/m damage level.

DOI: 10.54254/2753-8818/2026.33628

3.1. Applications based on MZI

The MZI is a natural architecture for high-linearity intensity modulation, featuring a simple transfer function and an extremely wide response bandwidth. To monitor the transient voltage and large current for power grids, the MZI sensor can perform non-contact monitoring of steady voltage and transient voltage for power grids. In 2021, Yang proposed an integrated MZI high current sensor with multi-loop antennas for achieving accurate measurement of pulsed high current in a range of 100 A–3300 A for high-fidelity waveform acquisition for non-intrusive diagnostic testing of power grid faults [7].

Moreover, for high-power threats, such as NEMP and HPM, MZI sensors based on TFLN have a high damage limit. In 2024, Qiu proposed a single-antenna TFLN-MZI sensor that was able to measure a maximum field strength of 726 kV/m and had a 3 dB bandwidth of 0.01 GHz to 27.5 GHz [1]. Additionally, in 2025, Hai has proposed a broadband MZI sensor with conical antenna arrays specially designed to capture high-power transient pulses and realized nanosecond response speed [3]. In the EMC test of 5G/6G communication equipment, MZI sensors are used to precisely detect high frequency microwave radiation inside a chip or in free space. In 2020, Zhang reported an IOES based on an unbalanced MZI sensor capable of working above 26 GHz with the minimum detectable field of 0.245 V/m [5].

3.2. Applications based on MI

MI is an important structure for integrated optical electric field sensors, where its core structure feature is its reflective. MI structure folds the optical path. It will travel twice along sensing arm by coating highly reflective film or a waveguide Bragg grating (WBG) at the end of the waveguide to complete reflection. Compared with the MZI, the MI structure can greatly increase the voltage sensitivity of the system, and its structure can make the system miniaturized level-integrated by doubling the effective electro-optic interaction length of the same physical device dimension. MI is especially effective for local metrology of high density and other geometrically confined geometries.

As an inherent single-ended architecture, the MI architecture is especially suitable for multi-dimensional vector detection. In 2014, Zhang combines three MI sensing units on a triangular prism to achieve the simultaneous detection of omnidirectional spatial components [5]. Later, in 2023, Liu proposed a broadband 3D electric field sensor based on TFLN platform and used reflective optical folding to image the complicated electromagnetic environment [1]. On the TFLN platform, MI sensors have continued to evolve towards very high sensitivity requirements. In 2022, Liu proposed an electrodeless MI sensor on TFLN, in which the rotation-shaped sensing arms were used to prolong the effective electro-optical interaction length, enabling high-fidelity signal transduction in sub-millimetre-sized sensing area [5].

Further efforts on a reflective MI sensor built on bulk LN can also provide a reliable way to retain the stable operating point of MI sensors in weak electromagnetic environments. In 2024, Qiu proposed a design of MI waveguide with asymmetry combined with a wavelength tuning feedback, and it is possible for the sensor to retain the stable linear operating point when in a surrounding environment with temperature changes [1]. It can keep the phased-bias locking and realize high-precision signal acquisition in environmental temperature change situations.

DOI: 10.54254/2753-8818/2026.33628

3.3. Applications based on MRR

While MRR makes use of the high-Q microcavity resonance to enhance the effective electro-optic interaction length, and they are the architectures of choice for metrology schemes for which detection limits in the range of μV/m are desired with a sensing volume of a sub-millimetre. The MRR structure can confine the optical energy in a micrometre-scale modal volume size for local acquisition of bioelectric potential or micro-electronic parasitic emissions. In 2021, Goncharenko presented a polymer-filled Si-based double-slot waveguide MRR structure with a minimum detectable electric field of 150 V/m [5]. Furthermore, in 2024, Babayigit presented a synaptic sensor based on a lithium niobate MRR which could detect the neural action potentials with amplitudes as low as 15 μV and high spatial resolution [8].

Another method to overcome the sinusoidal nonlinearity of the transfer function of MZI is to use linearized structures, such as Ring-Assisted Mach–Zehnder Interferometer (RAMZI/RMZI). In 2013, Cardenas presented a linearized silicon modulator based on the RMZI structure, to cancel the intermodulation distortion of the third order [5]. Extending this linearization concept to high refractive index contrast platforms, in 2024, Ke presented a Slot-Track RAMZI sensor, which was covered by electro-optic polymer films, and the third-order intermodulation distortion was able to be counteracted, enhancing the linear dynamic range and sensitivity for correctly tracking high-quality waveforms of strong transient fields at μs time-scale in smart grids environment [9].

3.4. Applications of other integrated optical structures

Other than MZIs, MIs and MRRs, various other diverse integrated architectures are significant alternative choices for various specialized metrology needs. For common-path interferometer (CPI), field-to-optical transduction effect can be obtained by using the birefringence effect in anisotropic crystals. For CPI, the two optical paths are common, so these CPI interferometers have inherent common-mode rejection for thermal fluctuations. In 1995, Jaeger proposed an integrated CPI high-voltage sensor worked in a harsh outdoor environment of substation. Later, in 2012, Wang proposed a new design to further improve the performance of CPI sensors applied in power system measurement [10]. Photonic crystal (PhC) structures have unique properties in sub-wavelength light confining. In 2020, Ma proposed a TFLN photonic crystal nanobeam structure that locates electromagnetic energy in high-Q nanobeam microcavities to realize an ultra high electric field sensing sensitivity of 0.15 V/m to facilitate high resolution localized measurements of field distributions inside the microelectronic circuits [5].

Fabry-Perot (FP) resonant cavities exploit a resonance peak shift or cavity length change to detect electric field. For instance, in 2023, Wang proposed an intense electric field sensor based on an FP interferometric resonator employing lithium niobate crystals to measure the strong electrostatic field or HV pulse [5]. In 2024, in order to further increase the sensitivity of this kind of sensor, Wang proposed an ultrasensitive sensor exploiting the harmonic Vernier effect in a cascaded FP cavity, and the detection limit could be pushed to the MV/m range for capturing lightning-induced pulses [11].

3.5. Comprehensive comparison of MZI, MI and MRR sensing structures

Discussion of the technical trade-offs among various sensing architectures for integrated optical waveguide electric field sensor structures. For this purpose, this paper compares different waveguide electric field sensors across prominent performance metrics such as structure, modulation sensitivity, bandwidth and stability to environment. As summarized in Table 1, MZI is the standard and typical

DOI: 10.54254/2753-8818/2026.33628

architecture of high-linearity intensity modulation with the best existing bandwidth performance and its transfer function is also a simple cosine form, which allows easy extraction of electric field intensity from optical response. The Michelson structure is distinct from the above with its reflective design in which the optical signals propagate back and forth in the sensing arm, which produces twice optical path difference and optical phase response at the same sensing physical length, easily realizable miniaturization of device for high-fidelity operation in compact spaces.

Compared with the former two types of interferometric structures, MRR takes advantage of the high-Q microcavity resonance. It obtains the resonant enhancement effect by multi circulating of light in the ring, realizes excellent field detection limit with a very small sensing spot. But MRR is very sensitive to ambient temperature and humidity fluctuations and is limited by the steep Lorentzian characteristics of the transmission profile of resonance modes, so it working bandwidth is usually quite narrow. Table 1 is the Performance Comparison of Integrated Optical Electric Field Sensor based on MZI, MI and MRR.

Table 1. Performance Comparison of Integrated Optical Electric Field Sensors based on MZI, MI and MRR

Comparison dimensions	MZI	MI	MRR
working principle	Interference with phase difference between two arms	Reflective two-arm phase difference interference	resonance wavelength drift
modulation efficiency	standard efficiency	High (optical path doubled)	Extremely High (Resonance Enhancement)
Chip size	Larger (branch structures occupy space)	Medium (single-ended packaging is relatively compact)	Extremely small (micrometer scale)
response bandwidth	Ultra-wideband (up to GHz level)	broadband	Narrow (limited by resonance points)
transfer function	Simple (cosine function), easy to demodulate	Simple (cosine function)	Complex (Lorenz-type), with strong nonlinearity
stability	Good (compensated through asymmetric design)	Relatively good (relatively uniform single-ended heat dissipation)	Poor (extremely susceptible to temperature fluctuations)
Typical applications	Ultra-wideband, high-field, EMP monitoring	3D vector detection, miniaturized weak field detection	Precision weak-field detection and biosensing

The comparative analysis leads to the following guidelines for sensor design:

For ultra-broadband response and high dynamic range (such as intense electromagnetic pulse monitoring), the MZI structure should be prioritized. When constrained by a narrow installation space and requiring high-sensitivity response, the MI structure is an ideal alternative. For application scenarios with extreme requirements for sensitivity and chip integration (such as on-chip microelectronic environment detection), the MRR exhibits greater potential, although complex operating point stability control circuits need to be additionally considered.

4. Challenges and future prospects

Although IOES has made remarkable progress in ultra-wideband response, electromagnetic interferences resistance, miniaturization, etc., it still has lots of challenges for practical engineering application and room for performance breakthrough. Facing the latest research results, future focus

DOI: 10.54254/2753-8818/2026.33628

of progress includes further improving stability, achieving full integration, obtaining multidimensional detection.

4.1. Core technical challenges

The DC drift nature of the use of LN material is the feature faced by IOES. Fluctuation of ambient temperature (pyroelectric and thermo-optic effects), the photorefractive effect and packaging stress all of them would make the operating point of the interferometer shift, and resulting nonlinear distortion of the test signal. To resist such impact, a number of feedback control systems, based on wavelength tuning, have been proposed. Long term robust operating point stability and DC drift performance of IOES against extreme temperature still need verification. Currently, the main optical electric field sensors measure alternating electric field by Pockels effect. Accurate measurement of DC electric fields remains to be solved as the following issues still exist: (i) the intensity of output light contains a DC component; (ii) the electro-optic crystal responds slowly to DC electric fields; and (iii) space charge effect affects measurement.

Technique for the fabrication of TFLN is also a challenge. Though TFLN has high integration capability, its ICP etching process has many strong restrictions. The roughness and inclination angle of etched side walls can directly influence the transmission loss and extinction ratio of the waveguide. At present, the extinction ratio of the TFLN device (often ranging from 8 to 12 dB) is generally less than that of bulk material devices (>30 dB), and hence, the signal-to-noise ratio of a sensor is limited.

4.2. Prospects for future development

Most existing sensors perform unidirectional (scalar) measurements. A future research trend is to integrate three mutually orthogonal sensing units (such as those sensing Ex, Ey, Ez respectively) on a single chip, and realize omnidirectional accurate measurement of spatial electric field vectors with advanced decoupling algorithms. This is of great significance for locating interference sources and analyzing complex electromagnetic environments.

At present, the IOES system still relies on external laser sources and detectors. The future goal is to use heterogeneous integration technology to integrate lasers, optical amplifiers, interferometric sensing units and photodetectors all on the same chip (PIC). Through 3D integrated packaging, the overall size is further reduced, costs are lowered and link loss is minimized.

With the development of 5G/6G communications, the demand for electric field sensing in bands above 30 GHz and even the THz band has become increasingly urgent. To mitigate high-frequency signal roll-off, electrode architectures must integrate velocity matching designs [12].

Software-defined intelligent perception, leveraging algorithms like Random Forest (RF), enables precise real-time calibration of the sensor operating point. For example, improved wavelength tuning algorithms with logarithmic operations or 3 dB bandwidth point locking could eliminate interference from laser power fluctuations, to suppress environmental noise and fit nonlinear mapping relationships in complex electromagnetic environments.

5. Conclusion

This work synthesizes the fundamental mechanisms, material advancements, and diverse implementation schemes of integrated optical waveguide electric field sensing technology. IOES represent indispensable metrology techniques for power grid diagnostics and EMC assessment,

DOI: 10.54254/2753-8818/2026.33628

owing to their all-dielectric composition and inherent electromagnetic transparency, ultra-wide response bandwidth (theoretically up to the THz range), and near-zero disturbance to the original electric field. High-fidelity linear detection is governed by the Pockels effect of electro-optic crystals, which converts spatial electric fields into optical phase modulation through interferometric or resonant structures. The technology is shifting toward high-refractive-index-contrast TFLN platforms, migrating from traditional Bulk LN. TFLN has reduced device dimensions from the centimeter to the millimeter scale while significantly enhancing modulation efficiency and bandwidth, with experimental ultra-wideband responses reaching up to 27.5 GHz. Regarding structural characteristics, the MZI is the most mature for high-power monitoring; the MI enhances modulation efficiency, doubles the optical path difference and enables compact single-ended integration, and the MRR demonstrates great potential for extreme sensitivity. Furthermore, to address the inherent DC drift and environmental stability challenges, the implementation of asymmetric arm-length waveguides combined with wavelength tuning provides a robust methodology for phase-bias locking to ensure long-term stability at the quadrature point.

References

[1] L. Qiu, "Ultra-wideband Electric Field Sensing Technology Based on Thin Film Lithium Niobate, " M.S. thesis, Dept. Optoelectronic Sci. Eng., Univ. Electron. Sci. Technol. China, Chengdu, China, 2024.

[2] Tian, Yumo, Shuguo Xie, Shenshen Luan, Zixian Guo, Shenda Zhang, and Yan Yang. "Broadband High-Sensitivity Thin-Film LiNbO3 Based E-Field Sensor With LF-Shaped Electrode." IEEE Electron Device Letters 44, no. 9 (2023): 1555–58. https: //doi.org/10.1109/LED.2023.3299966.

[3] X. Hai, X. Zhang, X. Li, J. Zhou, and J. Li, "Broadband Integrated Optical Waveguide Electric Field Sensor for High-Power Transient Electromagnetic Pulse Measurement, " Transactions of China Electrotechnical Society, vol. 40, no. 17, Sep. 2025, doi: 10.19595/j.cnki.1000-6753.tces.241681.

[4] J. Zhang, X. Wang, and F. Chen, "Research and development of an integrated optical waveguide sensor for measurement of the explosive radiation electromagnetic pulse, " Chinese Journal of Scientific Instrument, vol. 43, no. 7, pp. 149–156, 2022.

[5] Z. Zhang, J. Zong, W. Qin, S. Li, J. Hu and J. He, "Advanced Optical Electric Field Sensor, " in CSEE Journal of Power and Energy Systems, 2024, doi: 10.17775/CSEEJPES.2024.08360.

[6] Umemoto, Takahiro, Masamitsu Sakuma, Yasuhito Hashiba, et al. "Development of Optical Voltage Transformer Using Electro-Optic Pockels Effect for HVDC Transmission Systems." IET Conference Proceedings 2023, no. 46 (2025): 1185–91. https: //doi.org/10.1049/icp.2024.0783.

[7] D. Yang, J. Zhang, F. Chen, Z. Zhao, and Y. Li, "Lithium niobate integrated MZI optical waveguide high current sensor, " Chinese Journal of Scientific Instrument, vol. 42, no. 11, pp. 87–95, 2021.

[8] Babayigit, Ceren, Rahim Esfandyarpour, and Ozdal Boyraz. "LiNbO3 -Based Synaptic Sensors via Microring Resonator Modulators." IEEE Sensors Journal 24, no. 13 (2024): 20280–88. https: //doi.org/10.1109/JSEN.2024.3402152.

[9] Ke, Kun, Qing Yang, Ning Chen, Ziyang Zhang, Xueqiong Zhu, and Zhen Wang. "Slot-Track Micro-Ring Assisted Mach-Zender Interferometric Optical Electric Field Sensor." Journal of Lightwave Technology 42, no. 19 (2024): 6981–92. https: //doi.org/10.1109/JLT.2024.3409580.

[10] Qian, Bo, Yang Xu, Yongsen Sun, Tianxi Xie, Yuchen Zhu, and Huaiyuan Yang. "Application of Integrated Optical E-Field Sensor for Non-Contact Transient Voltage Measurements." 2024 4th International Conference on Smart Grid and Energy Internet (SGEI), December 13, 2024, 497–501. https: //doi.org/10.1109/SGEI63936.2024.10914178.

[11] Jing, Guanghui, Tingting Wu, Jian Wen, et al. "All-Inorganic Perovskite $CsPbBr_3$-Assisted Mach-Zehnder Interferometer (MZI) Optical Fiber Sensor for Highly Sensitive Ultraviolet and Blue Light Detection." Optics and Lasers in Engineering 201 (June 2026): 109676. https: //doi.org/10.1016/j.optlaseng.2026.109676.

[12] W. Xu, L. Zhou, and J. Chen, "Silicon-Based Waveguide Integrated Optical Phased Array Chips for LiDAR: Design Challenges and Breakthroughs (Invited), " Acta Optica Sinica, vol. 44, no. 15, p. 1513026, 2024.